Polyhedron 31 (2012) 379–385

Contents lists available at SciVerse ScienceDirect

Polyhedron

journal homepage: www.elsevier.com/locate/poly

Supramolecular networks of Mn(III)–Schiff base complexes assembled by nitrate counterions: X-ray crystal structures of 1D chains and 2D networks

M. Ángeles Vázquez-Fernández [a], M. Isabel Fernández-García [a,*], Ana M. González-Noya [a], Marcelino Maneiro [a,*], Manuel R. Bermejo [b], M. Jesús Rodríguez-Doutón [c]

[a] Departamento de Química Inorgánica, Facultade de Ciencias, Universidade de Santiago de Compostela, Avda. Alfonso X, Lugo E-27002, Spain
[b] Departamento de Química Inorgánica, Facultade de Química, Universidade de Santiago de Compostela, Santiago de Compostela E-15782, Spain
[c] Department of Chemistry and INSTM Research Unit, University of Modena and Reggio Emilia, Via G. Campi 183, 41100 Modena, Italy

ARTICLE INFO

Article history:
Received 28 July 2011
Accepted 25 September 2011
Available online 1 October 2011

Keywords:
Manganese complexes
Schiff bases
Supramolecular structure
Crystal structure
Hydrogen bonds

ABSTRACT

A series of Mn(III) nitrate complexes have been synthesized from dianionic hexadentate Schiff bases obtained by condensation of 3-methoxy-2-hydroxybenzaldehyde with different diamines. The complexes have been characterised by elemental analysis, ESI mass spectrometry, IR and ^{1}H NMR spectroscopy. Magnetic studies and molar conductivity measurements were also performed. Complexes $[MnL^1(H_2O)_2]_2\cdot 2NO_3\cdot 2CH_3OH$ (**1**), $[MnL^2(H_2O)_2]_2\cdot 2NO_3\cdot 2CH_3OH$ (**2**) and $[MnL^5(H_2O)_2]_2\cdot 2NO_3\cdot 6H_2O$ (**5**) were crystallographically characterised. The X-ray structures show an octahedral geometry around the metal with the Schiff base in the equatorial plane acting as tetradentate and water or methanol molecules in the axial positions. The octahedron entities are linked in pairs by μ-aquo bridges between neighbouring axial water molecules and also by π–π stacking interactions, establishing dimeric and polymeric structures. Nitrate anions are accommodated in the cavities of the framework and form hydrogen bonds with the aqua ligands and the methanol or crystal water, leading to infinite supramolecular aggregates of the complexes. Comparison of chloride, perchlorate and nitrate complexes indicate that the nature of the anions is the key factor directing the structural topologies.

1. Introduction

The design and synthesis of supramolecular architectures sustained by noncovalent intermolecular forces (hydrogen bonding, π–π stacking,...) represents a rapidly expanding field that offers potential for the development of new types of functional solids [1–4]. The self-assembly of metal–organic frameworks is highly influenced by factors such as the geometric requirements of metal ions [5,6], the ligand design [7,8], the solvents used for crystallisation [9] or the selection of the counteranions [10,11]. The management of all these factors makes it possible to know the synthetic strategies that lead to the desired species with predictable structures and properties. However, establishing the general and precise principles of constructing desirable framework topologies is still a large challenge. In particular, the role of anions in self-assembly processes has emerged as an increasingly active theme [12,13]. Our recent efforts on controlled coordination-driven self-assembly of Mn–Schiff complexes also shed some lights on this point.

For years, the coordination chemistry of manganese was focused on the active role of this metal ion in many redox enzymes [14,15], but the supramolecular arrangements of manganese complexes have been less studied. Most recently, with the skill and the motivation acquired due to our successes in the construction of well-appealing supramolecular architectures [7,16,17], we are investigating the overlooked supramolecular arrangements of manganese(III) complexes. Our scheme consists of obtaining the aggregation of discrete manganese(III) complexes into multidimensional arrays through metal-free self-assembly, using Schiff base ligands with hydroxyl groups in adequate positions. Thus, we have already reviewed the supramolecular arrangements with carboxylate groups [18], chloride [19] and perchlorate [20] counterions. The hydrogen bonding net led to supramolecular systems with different dimensionality where the counterion plays a crucial role. In this paper we describe the results of our research work with the nitrate anion.

There are few examples of Mn(III)–Schiff base (or porphyrin) complexes with the nitrate anion. Of those found in the literature some of them incorporate the ion to the first coordination sphere [21]; the nitrate group may also be bridging manganese ions in Mn–carboxylate complexes [22], but there a small number of cases where the nitrate acts as counterion in this type of systems [23,24]. Moreover, even these publications do not discuss the

---

* Corresponding authors. Tel.: +34 982824065; fax: +34 982285872 (M. Maneiro).

E-mail addresses: misabel.fernandez.garcia@usc.es (M. Isabel Fernández-García), marcelino.maneiro@usc.es (M. Maneiro).

0277-5387/$ - see front matter © 2011 Elsevier Ltd. All rights reserved.
doi:10.1016/j.poly.2011.09.031

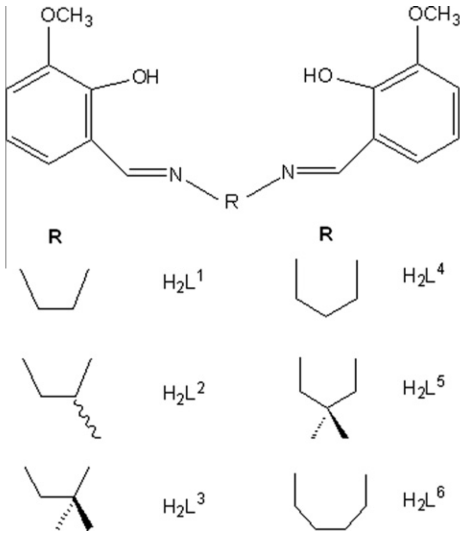

Scheme 1.

supramolecular arrangements of these complexes. We have also previously added nitrate groups to Mn(III)–Gd(III)–Schiff base complexes but this anion stabilised joining the Gd [25].

The ability of these anions for establishing hydrogen bonds would lead to new supramolecular architectures and would also lead to systems of interest for the selective recognition between anions and receptors [26–28]. Now we report a series of Mn(III)–Schiff-base complexes associated by nitrate counteranions, using ligands with suitable OH groups. The key role of anions in tuning the resultant structural topologies has been concluded. The selected Schiff-base ligands, H_2L^n (see Scheme 1) are the result of the condensation of 3-methoxy-hydroxybenzaldehyde with diverse diamines (1,2-diaminoethane for H_2L^1; 1,2-diamino-2-methylethane for H_2L^2; 1,2-diamino-2,2-dimethylethane for H_2L^3; 1,3-diaminopropane for H_2L^4; 1,3-diamino-2,2-dimethylopropane for H_2L^5 and 1,4-diaminobuthane for H_2L^6). H_2L^1–H_2L^6 contain six potential donor atoms, two imine nitrogen atoms and two phenol oxygen atoms in an inner compartment and two outer methoxy groups.

2. Material and methods

2.1. Materials

All the starting materials (Aldrich) and solvents (Probus) used for the synthesis were of commercially available reagent grade and were used without further purification.

2.2. Physical measurements

Elemental analyses were performed on a Carlo Erba Model 1108 CHNS–O elemental analyzer. The IR spectra were recorded as KBr pellets on a Bio-Rad FTS 135 spectrophotometer in the range 4000–400 cm^{-1}. ^1H and ^{13}C NMR spectra were recorded on a Bruker AC-300 spectrometer using DMSO-d_6 (296 K) as solvent and $SiMe_4$ as an internal reference. The electro-spray mass spectra of the compounds were obtained on a Hewlett–Packard model LC-MSD 1100 instrument (positive ion mode, 98:2 CH_3OH–HCOOH as mobile phase, 30–100 V). Room-temperature magnetic susceptibilities were measured using a digital measurement system MSB-MKI, calibrated using mercury tetrakis(isothiocyanato)cobaltate(II) $Hg[Co(NCS)_4]$ as a susceptibility standard. Variable-temperature magnetic data were obtained with a Quantum Design MPMS SQUID susceptometer. Sample was a 3 mm diameter pellet moulded from ground crystalline sample. Electronic spectra were recorded on a Cary 230 spectrometer. Conductivities of 10^{-3} M solutions in DMF were measured on a Crison microCM 2200 conductivimeter.

2.3. Preparation of the Schiff base ligands

All the Schiff bases used in this study were prepared by condensation of the appropriate diamine with 3-methoxy-2-hydroxybenzaldehyde. H_2L^1–H_2L^5 have been already reported and characterised by standard techniques [20,29,30]. H_2L^6 was prepared by the method outlined below and satisfactorily characterised by elemental analysis, ^1H- and ^{13}C NMR and IR spectroscopy, and ESI mass spectrometry.

2.3.1. H_2L^6

To a methanolic solution (100 mL) of 1.00 g (6.57 mmol) of 3-methoxy-2-hydroxybenzaldehyde (1.00 g, 6.57 mmol) was added 1,4-diaminobutane (0.33 mL, 3.29 mmol). The mixture was refluxed for 3 h in a round bottom flask fitted with a Dean-Stark trap to remove the water produced during the reaction. After, the solution was concentrated to yield a yellow solid that was collected by filtration, washed with diethyl ether and dried in vacuo. Yields were almost quantitative. M.p. 143 °C. *Anal.* Calc. for $C_{20}H_{24}N_2O_4$ (356.4): C, 67.4; H, 6.8; N, 7.9. Found: C, 67.3; H, 6.8; N, 7.8%. MS ESI (*m/z*): 357. IR (KBr, cm^{-1}): ν(O–H) 3099 (m), ν(C=N) 1629 (vs), ν(C–O) 1245 (s). ^1H NMR (DMSO-d_6, ppm): δ 1.73 (q:quintuplet, 4H), 3.65 (t, 4H), 3.77 (s, 6H), 6.77 (t, 2H), 6.99 (d, 2H), 7.01 (d, 2H), 8.53 (s, 2H), 13.90 (br). ^{13}C NMR (DMSO-d_6, ppm): δ 27.9 ($-CH_2-$), 55.7 ($=N-CH_2-$), 57.0 ($-OCH_3$), 114.6–123.2 (*C*ar), 148.1 (*C*–OH), 152.4 (*C*–OCH_3), 165.9 (*C*=N).

2.4. Complex preparation

All the manganese(III) Schiff base complexes were prepared by stirring a methanol solution (50 mL) of the corresponding ligand and adding subsequently a methanol solution (30 mL) of $Mn(NO_3)_2\cdot 4H_2O$ at room temperature. The initial light colour of the solutions rapidly changed to brown. After 3 h of stirring at room temperature slow evaporation of solvent lead to deposition of brown compounds. The products were collected by filtration, washed with diethyl ether (2 × 20 mL) and then dried *in vacuo*. Yields of the complexes vary, but are typically of the order of 70%.

2.4.1. $[MnL^1(H_2O)_2]\cdot NO_3\cdot CH_3OH$, (**1**)

H_2L^1 (0.33 g, 1.00 mmol); $Mn(NO_3)_2\cdot 4H_2O$ (0.26 g, 1.00 mmol); yield: 0.36 g (70%). *Anal.* Calc. for $C_{19}H_{26}MnN_3O_{10}$ (511.4): C, 44.6; H, 5.1; N, 8.2. Found: C, 44.5; H, 4.9; N, 8.3%. MS ESI (*m/z*): 381 $[MnL^1]^+$, 824 $[Mn_2L^1_2(NO_3)]^+$. IR (KBr, cm^{-1}): ν(O–H) 3420 (m), ν(C=N) 1619 (vs), ν(C–O) 1257 (s), $\nu(NO_3)$ 1384 (vs), 830 (m), 738 (s). ^1H NMR (DMSO-d_6, ppm): δ −30.52 (H4), −21.50 (H5). μ = 5.1 BM. Λ_M = 81 μS.

2.4.2. $[MnL^2(H_2O)_2]\cdot NO_3\cdot CH_3OH$, (**2**)

H_2L^2 (0.20 g, 0.58 mmol); $Mn(NO_3)_2\cdot 4H_2O$ (0.15 g, 0.58 mmol); yield: 0.23 g (75%). *Anal.* Calc. for $C_{20}H_{28}MnN_3O_{10}$ (525.4): C, 45.7; H, 5.4; N, 8.0. Found: C, 45.4; H, 5.1; N, 8.0%. MS ESI (*m/z*): 395 $[MnL^2]^+$, 852 $[Mn_2L^2_2(NO_3)]^+$. IR (KBr, cm^{-1}): ν(O–H) 3415 (m), ν(C=N) 1619 (vs), ν(C–O) 1254 (s), $\nu(NO_3)$ 1384 (vs), 859 (m), 735 (s). ^1H NMR (DMSO-d_6, ppm): δ −27.77 (H4), −17.50, −18.95 (H5). μ = 5.0 BM. Λ_M = 72 μS.

2.4.3. $[MnL^3(H_2O)_2].NO_3.H_2O$, (**3**)

H_2L^3 (0.20 g, 0.56 mmol); $Mn(NO_3)_2\cdot 4H_2O$ (0.14 g, 0.56 mmol); yield: 0.19 g (65%). *Anal.* Calc. for $C_{20}H_{28}MnN_3O_{10}$ (525.4): C, 45.7; H, 5.4; N, 8.0. Found: C, 45.8; H, 5.2; N, 8.2%. MS ESI (*m/z*): 409 $[MnL^3]^+$, 880 $[Mn_2L^3{}_2(NO_3)]^+$. IR (KBr, cm^{-1}): ν(O–H) 3415 (m), ν(C=N) 1608 (vs), ν(C–O) 1257 (s), $\nu(NO_3)$ 1384 (vs), 860 (m), 737 (s). ^1H NMR (DMSO-d_6, ppm): δ −27.94 (H4), −17.40, −18.80 (H5). μ = 5.0 BM. Λ_M = 71 µS.

2.4.4. *$[MnL^4(H_2O)_2].NO_3.2H_2O$, (**4**)*

H_2L^4 (0.25 g, 0.73 mmol); $Mn(NO_3)_2{\cdot}4H_2O$ (0.18 g, 0.73 mmol); yield: 0.29 g (75%). *Anal.* Calc. for $C_{19}H_{28}MnN_3O_{11}$ (529.4): C, 43.1; H, 5.3; N, 7.9. Found: C, 42.9; H, 5.0; N, 7.9%. MS ESI (*m/z*): 395 $[MnL^4]^+$, 852 $[Mn_2L^4{}_2(NO_3)]^+$. IR (KBr, cm^{-1}): ν(O–H) 3425 (m), ν(C=N) 1613 (vs), ν(C–O) 1253 (s), $\nu(NO_3)$ 1384 (vs), 860 (m), 735 (s). ^1H NMR (DMSO-d_6, ppm): δ −20.97 (H4), −16.28 (H5). μ = 4.8 BM. Λ_M = 72 µS.

2.4.5. *$[MnL^5(H_2O)_2].NO_3.3H_2O$, (**5**)*

H_2L^5 (0.25 g, 0.68 mmol); $Mn(NO_3)_2{\cdot}4H_2O$ (0.18 g, 0.68 mmol); yield: 0.29 g (79%). *Anal.* Calc. for $C_{21}H_{32}MnN_3O_{11}$ (557.4): C, 45.2; H, 5.8; N, 7.5. Found: C, 45.3; H, 5.7; N, 7.5%. MS ESI (*m/z*): 423 $[MnL^5]^+$, 908 $[Mn_2L^5{}_2(NO_3)]^+$. IR (KBr, cm^{-1}): ν(O–H) 3427 (m), ν(C=N) 1609 (vs), ν(C–O) 1254 (s), $\nu(NO_3)$ 1384 (vs), 850 (m), 739 (s). ^1H NMR (DMSO-d_6, ppm): δ −21.97 (H4), −18.00 (H5). μ = 5.3 BM. Λ_M = 68 µS.

2.4.6. *$[MnL^6(H_2O)_2]{\cdot}NO_3{\cdot}3H_2O$, (**6**)*

H_2L^6 (0.20 g, 0.56 mmol); $Mn(NO_3)_2{\cdot}4H_2O$ (0.14 g, 0.56 mmol); yield: 0.28 g (90%). *Anal.* Calc. for $C_{20}H_{32}MnN_3O_{12}$ (561.4): C, 42.8; H, 5.7; N, 7.5. Found: C, 42.4; H, 5.3; N, 7.4%. MS ESI (*m/z*): 409 $[MnL^6]^+$, 880 $[Mn_2L^6{}_2(NO_3)]^+$. IR (KBr, cm^{-1}): ν(O–H) 3438 (m), ν(C=N) 1612 (vs), ν(C–O) 1254 (s), $\nu(NO_3)$ 1384 (vs), 868 (m), 742 (s). ^1H NMR (DMSO-d_6, ppm): δ −26.23 (H4), −20.56 (H5). μ = 5.3 BM. Λ_M = 69 µS.

2.5. *Crystallographic data collection and refinement of the structures*

Single crystals of the complexes **1**, **2** and **5**, suitable for X-ray diffraction studies, were obtained by slow evaporation of the methanolic solution at room temperature.

Detailed crystal data collection and refinement for the complexes are summarised in Table 1. Intensity data were collected on a Bruker-Smart CCD-1000 diffractometer employing graphite-monochromated Mo Kα radiation (λ = 0.71073 Å) for **2** at room temperature, and for **5** at 180 K. Data for **1** were collected at 180 K on a Stoe Imaging Plate Diffractometer System (IPDS) using a graphite monochromated Mo Kα radiation (λ = 0.71073 Å) and equipped with an Oxford Cryosystems cooler device. The structures were solved by direct methods [31] and finally refined by full-matrix least-squares base on F^2. An empirical absorption correction was applied using SADABS [32]. All non-hydrogen atoms were included in the model at geometrically calculated positions.

3. Results and discussion

The manganese(III) complexes **1**–**6** were prepared as detailed in the Section 2. They appear to be stable in the solid state and in solution, and they are moderately soluble in common organic solvents and soluble in polar aprotic coordinating solvents such as DMF and DMSO. Elemental analysis establishes their general formulae as $[MnL(H_2O)_2]{\cdot}NO_3{\cdot}x$Solv (Solv = H_2O or CH_3OH). These formulations are in agreement with molar conductivity measurements in 10^{-3} M DMF solutions, which are in the range 68–81 µS cm^{-1}, indicating behaviour attributable to 1:1 electrolytes [33]. Furthermore, other spectroscopic techniques support such formula and give insights into both solid and solution structure of the complexes.

Table 1
Crystal data and structure refinement for **1**, **2** and **5**.

Complex	**1**	**2**	**5**
Empirical formula	$C_{19}H_{26}MnN_3O_{10}$	$C_{20}H_{28}MnN_3O_{10}$	$C_{21}H_{32}MnN_3O_{11}$
Formula weight	511.37	525.39	557.44
T (K)	180(2)	293(2)	100(2)
Wavelength (Å)	0.71073	0.71073	0.71073
Crystal system	orthorhombic	triclinic	monoclinic
Space group	*Pbca*	$P\bar{1}$	*I*2/*a*
a (Å)	12.9621(11)	9.089(2)	25.7414(14)
b (Å)	14.2447(11)	12.048(3)	7.5727(4)
c (Å)	23.9115(15)	12.761(3)	27.682(2)
α (°)	90.00	114.036(4)	90
β (°)	90.00	108.147(4)	115.236(2)
γ (°)	90.00	91.751(4)	90
V (Å^3)	4415.0(6)	1192.6(5)	4881.0 (5)
Z	8	2	8
$D_{calc.}$ (g cm^{-3})	1.539	1.463	1.517
μ (mm^{-1})	0.659	0.612	0.606
$F(000)$	2128	548	2336
$\theta_{min/max}$ (°)	2.32/26.03	1.87/26.44	1.63/25.68
Total data	33158	13613	81746
Unique data	4312	4866	4631
R_{int}	0.0456	0.0238	0.0984
Restraints/parameters	6/311	6/330	11/371
Goodness-of-fit (GOF)	1.025	1.099	1.071
Final R indices $[I > 2\sigma(I)]$	R_1 = 0.0319 wR_2 = 0.0791	R_1 = 0.0499 wR_2 = 0.1503	R_1 = 0.0433 wR_2 = 0.0804
R indices (all data)	R_1 = 0.0418 wR_2 = 0.0840	R_1 = 0.0600 wR_2 = 0.1595	R_1 = 0.0730 wR_2 = 0.0884

All the complexes show similar IR spectra, exhibiting a strong band between 1619–1608 cm^{-1} characteristic of the ν(C=N) stretching mode, which is shifted 8–21 cm^{-1} lower with respect to the free Schiff base ligand, indicating the coordination to the manganese through the nitrogen atoms of the imine group. The band attributed to the ν(C–O) mode is shifted 4–10 cm^{-1} to higher frequencies with respect to the free ligand. These data suggest the coordination of the Schiff bases through the inner phenol oxygens and the imine nitrogen atoms. Strong bands centred at ca. 3400 cm^{-1} can be assigned to a combination of the ν(O–H) modes of coordinated and lattice water/methanol, now present in the complexes. The appearance of a new strong and sharp band at 1384 cm^{-1}, together with bands at ca. 740 and 850 cm^{-1} are characteristic of the presence of the non-coordinated nitrate counterion (see Supplementary data, Fig. S1) [34].

ESI mass spectra registered in methanol show peaks corresponding to the fragment $[MnL]^+$ for all the complexes, indicating the coordination of the Schiff base ligand to the metal centre. Other minor signals could be assigned to $[Mn_2L_2(NO_3)]^+$ units, which could be attributed to the presence of dimeric species (see Section 2 and also Supplementary data, Fig. S2).

3.1. *^1H NMR studies of the complexes*

Paramagnetic ^1H NMR studies of the complexes were registered using DMSO-d_6 as solvent, and the data serve to substantiate the formation of the manganese(III) complexes. The data interpretation was based on previous findings for manganese(III) complexes with related Schiff base ligands made by Pecoraro and co-workers [35] and on our own results [18,19]. The data are collected in the Section 2 and Fig. S3 of Supplementary data shows one of these spectra. The spectra contain between two and three upfield proton resonances, outside the diamagnetic region (δ = 0–14 ppm), due to the isotropically shifting of the ligand protons for high-spin manganese(III) complexes in an octahedral field. The signals must arise from the H4 and H5 protons of the aromatic phenoxy rings. The signals between −20.97 and −30.52 ppm arise from the H4 protons, while the resonances from −16.28 to −21.50 ppm arise from H5 protons. The signal corresponding to the H5 protons appears splitted in two in complexes including H_2L^2 and H_2L^3 Schiff bases; this fact can be attributed to the asymmetric nature of the Schiff base ligand of these complexes.

3.2. Electronic spectroscopic

The electronic spectroscopic data recorded are very similar for all compounds **1**–**6**, indicating that the Mn^{III} complexes are behaving as high-spin octahedral d^4 systems, suffering a Jahn–Teller distortion which affects the spectra and complicates its interpretation. A broad shoulder at about 520–600 nm ($\varepsilon = 120–500\ M^{-1}\ cm^{-1}$) is attributable to a d–d transition, while it is reasonable to assign the broad band obtained at 480–490 nm ($\varepsilon = 2600–3300\ M^{-1}\ cm^{-1}$) to the phenolate → Mn(III) charge-transfer.

The peak, appearing around 300 nm ($\varepsilon = 21\,000–23\,000\ M^{-1}\ cm^{-1}$), can be assigned to intraligand $\pi–\pi^*$. The energy and intensity of the LMCT and d–d transitions are in agreement with those reported for related Mn^{III} complexes [36–38].

3.3. Crystallographic studies

The structures of the complexes **1**, **2** and **5** have been crystallographically solved. Main crystallographic data for these complexes are summarised in Table 1, and bond lengths and angles are listed in Table 2.

In all cases the geometry around the manganese ion can be described as distorted octahedral. An ORTEP view of **5** with the atomic numbering scheme is shown in Fig. 1.

The coordination sphere around each manganese centre for **1**, **2** and **5** comprises the planar Schiff base ligand, tightly bound to the metal ion through the inner N_2O_2 compartment by the N_{imine} and O_{phenol} atoms ($Mn–N_{imine}$ bond lengths of 1.97–2.03 Å and $Mn–O_{phenol}$ of 1.87–1.90 Å, which are typical of such complexes and corroborate the bisdeprotonation of the ligands [19,20]), occupying the equatorial positions and giving rise to two six-membered chelate rings (which are nearly planar) and an additional five- or six-membered chelate ring (depending of the diamine R). The axial positions of the octahedron are occupied by capping water molecules in all cases. The Jahn–Teller elongation expected for d^4 high-spin manganese(III) appears outstanding in the axis orthogonal to the plane of the Schiff base ligand, with distances ranging from 2.20 to 2.32 Å, considerably longer than the equatorial Mn–O bond lengths quoted earlier. The deviation from an ideal octahedral geometry is also revealed by the range of angles observed around the metal centre (from 81.92° to 94.38°), as well as by the interaxial angle OW–Mn–OW of 170.10–178.70°.

Table 2
Selected bond lengths (Å) and angles (°) for the complexes **1**, **2** and **5**.

Complex	**1**	**2**	**5**
$Mn–O_p$	1.8718(12)	1.8774(18)	1.9026(16)
	1.8725(12)	1.8820(18)	1.9051(16)
$Mn–N_i$	1.9780(14)	1.978(2)	2.032(2)
	1.9783(14)	1.972(2)	2.029(2)
$Mn–O_{ax}$	2.2405(12)	2.257(2)	2.2040(18)
	2.3257(13)	2.263(2)	2.2063(19)
$O_p–Mn–O_p$	93.14(5)	94.38(8)	87.34(7)
$O_p–Mn–N_i$	91.63(5)	91.98(9)	89.63(7)
	92.06(6)	81.92(11)	89.29(7)
	174.38(6)	173.77(9)	176.63(8)
	175.18	173.64(9)	176.96(8)
N–Mn–N	83.16(6)	88.88(9)	93.74(8)
$O_a–Mn–O_a$	170.10(5)	178.70(10)	169.63(7)
Mn···Mn	4.736	4.876	5.082

$O_p = O_{phenolic}$; $N_i = N_{iminic}$; $O_a = O_{axial}$.

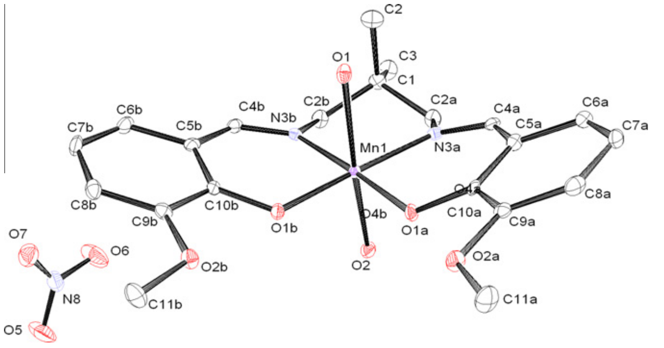

Fig. 1. An ORTEP view of the environment around the manganese centre for **5**, including the atomic numbering scheme. Thermal ellipsoids are drawn at the 50% probability level. Hydrogen atoms and aqua uncoordinated are omitted for clarity. This structure shows a boat-shaped conformation.

The differences between **1**, **2** and **5** arise from the superstructure of the complexes. All of them show associations via a combination of π-aryl offset interactions (3.71–3.89 Å) [39–40] and hydrogen bonds between capping water molecules and both phenoxy and methoxy oxygen atoms of the neighbouring Schiff base ligand. These hydrogen bonds are charge-assisted, that is, the hydrogen bond donor and/or acceptor carry positive and negative ionic charges, respectively, and hence they are rather strong and short [41]. As result of these supramolecular interactions, the Mn···Mn distances of about 4.7–5.1 Å are short for monomeric compounds, yielding $[MnL(Solv)_2]_2^{2+}$ dimers for **1** and **2** (being L Schiff base and Solv the water/solvent molecules), and $[MnL(Solv)_2]_n^{n+}$ polymers in **5**. The positions of the nitrate counterions and the uncoordinated methanol and water molecules are the determining factors to induce the resulting different crystal packing of these complexes:

(i) The $[MnL(Solv)_2]_2^{2+}$ μ-aquo dimers in **1** and **2** are electrostatically stabilised by nitrate counterions (Fig. 2). These anions are acting as hydrogen-bonding acceptors with coordinated water or methanol, interconnecting the μ-aquo dimers and enriching the final supramolecular structure.
  (a) In **2** the external apical water molecules of the dimers form two hydrogen bonds with two oxygen atoms of the nitrate group; one of them is also bound to a methanol molecule. Thus, there are two nitrate groups and two methanol molecules between μ-aquo dimers, generating a 1D chain (Fig. 3).
  (b) In the case of **1** an apical water molecule establishes two hydrogen bonds: to O8 of the nitrate group and to O10 of the methanol; the nitrate ion also establishes a hydrogen bond through the O9 to a different methanol molecule, which is bound to another apical water molecule of a neighbouring dimer. This supramolecular interaction originates a 2D net (Fig. 4).

(ii) The polymeric structure of **5** grows in one dimension, through hydrogen bonding between capping water molecules and both phenoxy and methoxy oxygen atoms of the neighbouring Schiff base ligand. In this case, nitrate groups and solvent water molecules are connecting through hydrogen bonds but they do not establish any of these interactions to the Mn–Schiff base moiety. This result in a 1D Mn–Schiff base chain, parallel to a channel made up of the nitrate counterions and the water molecules (Fig. 5). The disposition of the Schiff base ligand is not planar, and the two phenyl rings are located on the same side of the N_2O_2 coordination site

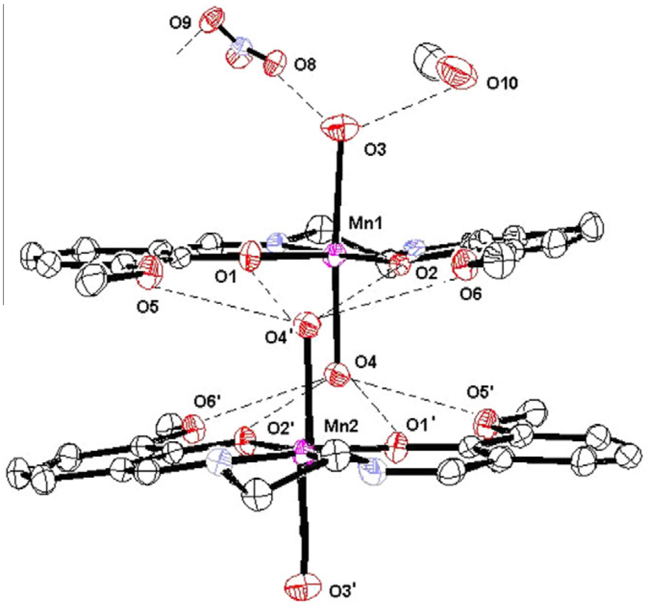

Fig. 2. Molecular structure of **1**.

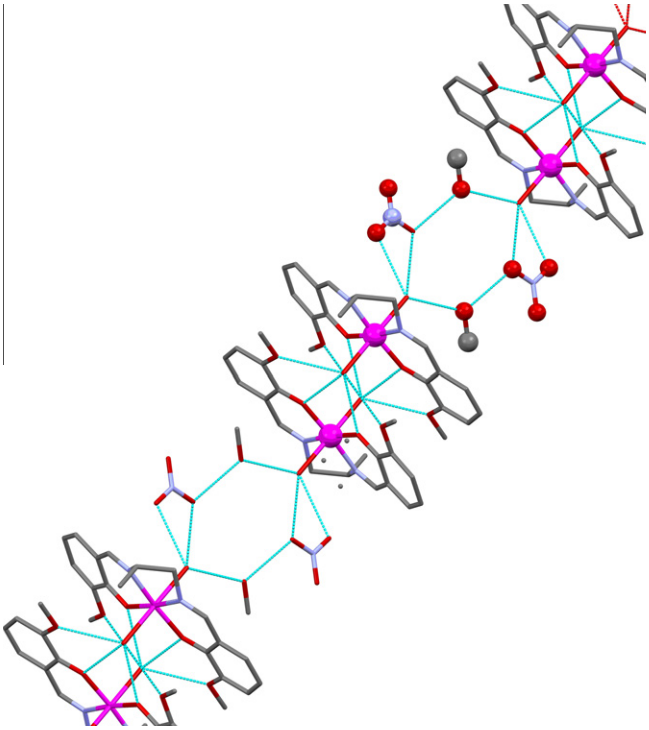

Fig. 3. View along the *c* axis of **2**, showing two nitrate groups and two methanol molecules between μ-aquo dimers, generating a 1D chain.

plane. The deviation from the Mn–N_2O_2 mean plane in such a way gives rise to a boat-shaped conformation, already observed in literature for similar cases [25].

3.4. Magnetic studies

Values for the $\chi_M T$ product of compound **1**–**6** at room temperature are very close to the spin-only value of 3 $cm^3\ mol^{-1}$ K expected for high-spin magnetically diluted d^4 manganese(III) ion.

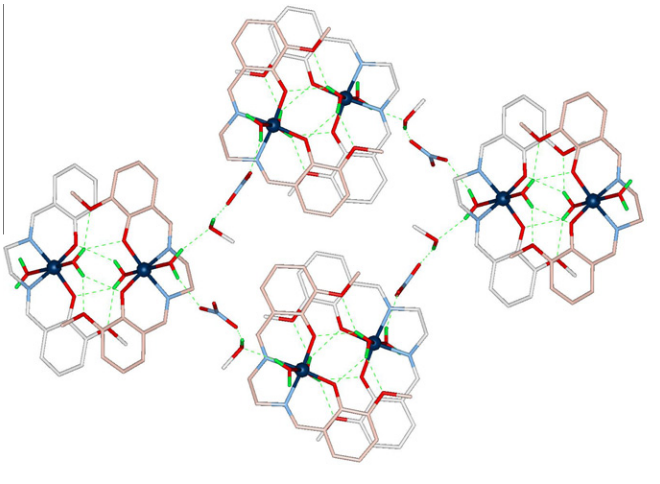

Fig. 4. Stick diagram for **1** showing the hydrogen bonding between adjacent $[MnL^1(H_2O)_2]_2^{2+}$ dimeric units through nitrate anions and methanol solvent molecules.

Magnetic studies at variable temperature have been done for **1** (between 150 and 2 K) in a 0.8 T applied magnetic field. The data obtained for complex **1** are collected in Table S1 of Supplementary data. Fig. 6 shows the thermal dependence of the $\chi_M T$ product per Mn_2 unit. The Curie–Weiss law is obeyed in the 15–150 K temperature range. At 150 K the $\chi_M T$ product is equal to 5.91 $cm^3\ mol^{-1}$ K, which is close to the room temperature value. As the temperature is lowered, the $\chi_M T$ is almost constant from 150 to 45 K, it decreases smoothly down to 14 K (2.54) and then more steeply, reaching a value of 0.55 $cm^3\ mol^{-1}$ K at 2 K. This behaviour is consistent with weak antiferromagnetic interactions and/or zero field splitting effects originating from the Mn(III) ion.

According to the X-ray structure of **1**, which consists of μ-aquo dimers (Fig. 2), the magnetic data were analysed by using a Hamiltonian that takes into account an isotropic coupling between Mn(1)–Mn(2) centres through the hydrogen bonds [42]. The estimation of the coupling constant was performed using the Hamiltonian $H = -JS_{Mn1}S_{Mn2} + D_{Mn}(S^2Mn_{z1} + S^2Mn_{z1})$, which includes the axial single-ion local anisotropy of the Mn(III) ions, according to the solved crystal structure. This model does not take into account any intermolecular interactions, since they are expected to be weaker than *J* because of significantly greater distances involved.

The best fit of the experimental susceptibility data with the above Hamiltonian led to the following parameters: $J = -0.46\ cm^{-1}$, $D = 2.48$, and the mean Landé factor $g = 2.016$. The *J* value, taking into account the magnetic exchange interaction through the pair of complementary hydrogen bonds, as well as the *D* value, are similar to those observed in other Mn(III)–Schiff base μ-aquo dimers with different counterions [29,42].

The solved crystal structures of **2** and **5** show a bridging scheme between the manganese(III) ions similar to **1**, through hydrogen bonding between capping water molecules and both phenoxy and methoxy oxygen atoms of the neighbouring Schiff base ligand. Previous magnetic studies on related compounds between 300 and 5 K also indicated little or no antiferromagnetic interaction between the metal centres [29,43,44]. The room temperature magnetic moments observed in this study do not give cause to suppose that any different magnetic behaviour should occur.

3.5. Anion control of the self-assembly

We have early published the behaviour of the chloride and perchlorate counterions as multiple hydrogen-bond acceptors for similar manganese(III)–Schiff base complexes. Thus, each chloride ion

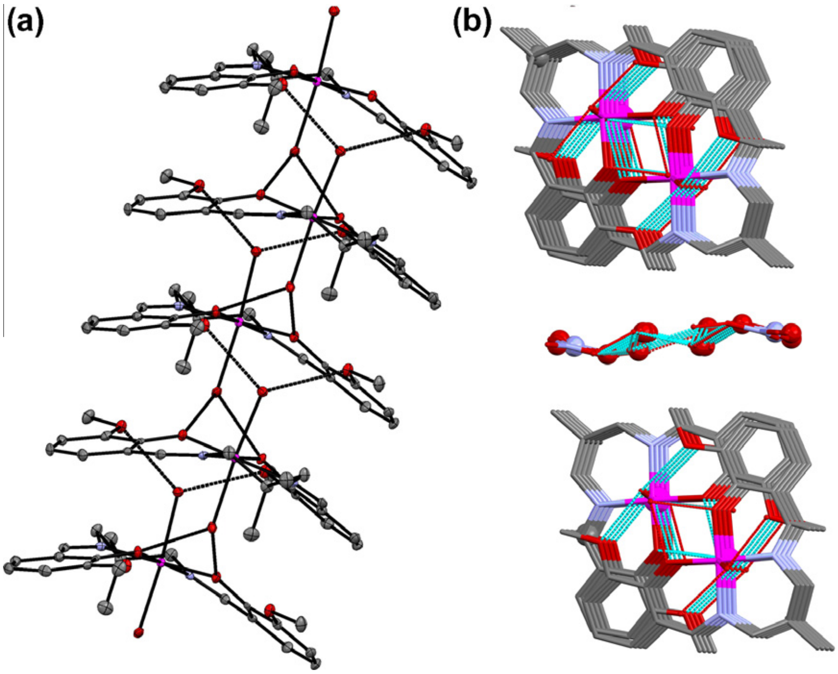

Fig. 5. (a) View along the *c* axis of the 1D chain of Mn(III) complexes for **5**; hydrogen atoms and uncoordinated nitrates and solvent water molecules are omitted for clarity; (b) packing view of **5** showing the 1D chains placing nitrates and solvent water molecules in channels.

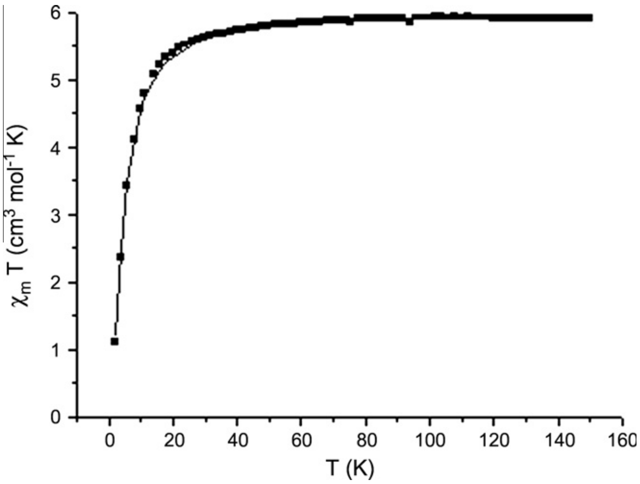

Fig. 6. Plot of $\chi_M T$ vs. temperature for **1** per Mn_2 unit.

could be involved in four O–H···Cl bonds, connecting three neighbouring cationic complexes and assembling them to constitute a 2D network [19]. The dimensionality of the supramolecular arrangement is reduced by the assembly through perchlorate counterions because each anion is able to form only two hydrogen bonds, directing preference to one direction and forming 1D chain [20].

The lower dimensionality can be interpreted in terms of the lower symmetry of the perchlorate (tetrahedral) than that of the chloride (spherical), involving a higher directionality of the network. This reasoning also justifies the behaviour of the nitrate groups in the present work. The lower symmetry of the trigonal planar nitrate anion also preferably induces 1D arrangement. This is the case of all the structures reported in this work but **1**, where the 2D network arises from the sum of the contacts due to the nitrate, methanol and water molecules.

4. Conclusions

This work again further emphasises the suitability of Schiff bases with inner and outer O–X (X = CH_3 in the present work) groups for establishing rich hydrogen-bonding networks. The results show that the nature of the counterion can control the architecture of final products in the self-assembly process by choosing more favourable noncovalent interactions in a cooperative manner. The dimensionality of the supramolecular array is affected by the nature of the anion which induces the assembly.

Acknowledgments

We thank Xunta de Galicia (09DPI004291PR and 10PXIB262132PR) for financial support.

Appendix A. Supplementary data

CCDC 785922, 785923 and 786041 contain the supplementary crystallographic data for **1**, **2** and **5**. These data can be obtained free of charge via http://www.ccdc.cam.ac.uk/conts/retrieving.html, or from the Cambridge Crystallographic Data Centre, 12 Union Road, Cambridge CB2 1EZ, UK; fax: (+44) 1223-336-033; or e-mail: deposit@ccdc.cam.ac.uk.. Supplementary data associated with this article can be found, in the online version, at doi:10.1016/j.poly.2011.09.031.

References

[1] J.M. Lehn, Supramolecular Chemistry: Concepts and Perspectives, Wiley-VCH, Germany, 1995.
[2] S. Leininger, B. Olenyuk, P.J. Stang, Chem. Rev. 100 (2000) 853.
[3] J. van Esch, Nature 466 (2010) 193.
[4] C.B. Aakeroy, N.R. Champness, C. Janiak, CrystEngComm. 12 (2010) 22.
[5] E.C. Constable, Chem. Commun. (1997) 1073.
[6] G.F. Swiegers, T.J. Malefetse, Coord. Chem. Rev. 225 (2002) 91.
[7] M.R. Bermejo, A.M. Gonzalez-Noya, R. Pedrido, M.J. Romero, M. Vazquez, Angew. Chem., Int. Ed. 44 (2005) 4182.
[8] M. Andruh, Chem. Commun. 47 (2011) 3025.

[9] M.R. Bermejo, M. Fondo, A.M. Gonzalez, O.L. Hoyos, A. Sousa, C.A. McAuliffe, W. Hussain, R. Pritchard, V.M. Novotorsev, J. Chem. Soc., Dalton Trans. (1999) 2211.

[10] R.L. Paul, Z.R. Bell, J.C. Jeffery, J.A. McCleverty, M.D. Ward, Proc. Natl. Acad. Sci. USA 99 (2002) 4883.

[11] L.P. Zhang, M. Du, W.J. Lu, T.C.W. Mak, Inorg. Chem. Commun. 8 (2005) 623.

[12] B. Notash, N. Safari, H.R. Khavasi, Inorg. Chem. 49 (2010) 11415.

[13] T. Ghosh, S. Das, S. Pal, Polyhedron 29 (2010) 3074.

[14] M. Maneiro, W.F. Ruettinger, E. Bourles, G.L. McLendon, G.C. Dismukes, Proc. Natl. Acad. Sci. USA 100 (2003) 3707.

[15] J. McEvoy, G. Brudvig, Chem. Rev. 106 (2006) 4455.

[16] M. Vazquez, A. Taglietti, D. Gatteschi, L. Sorace, C. Sangregorio, A.M. Gonzalez, M. Maneiro, R.M. Pedrido, M.R. Bermejo, Chem. Commun. (2003) 1840.

[17] R. Pedrido, M. Lopez, L. Sorace, A. Gonzalez-Noya, M. Cwiklinska, V. Suarez-Gomez, Chem. Commun. 46 (2010) 4797.

[18] M.R. Bermejo, M.I. Fernandez, A.M. Gonzalez-Noya, M. Maneiro, R. Pedrido, M.J. Rodriguez, J.C. Garcia-Monteagudo, B. Donnadieu, J. Inorg. Biochem. 100 (2006) 1470. and references therein.

[19] M.R. Bermejo, M.I. Fernandez, A.M. Gonzalez-Noya, M. Maneiro, R. Pedrido, M.J. Rodriguez, M. Vazquez, Eur. J. Inorg. Chem. (2004) 2769. and references therein.

[20] M.R. Bermejo, M.I. Fernandez, E. Gomez-Forneas, A. Gonzalez-Noya, M. Maneiro, R. Pedrido, M.J. Rodriguez, Eur. J. Inorg. Chem. (2007) 3789.

[21] H. Shyu, H. Wei, Y. Wang, Inorg. Chim. Acta 290 (1999) 8.

[22] G. Aromi, S. Bhaduri, P. Artus, K. Folting, G. Christou, Inorg. Chem. 41 (2002) 805.

[23] G. Morgan, K. Murnaghan, H. Muller-Bunz, V. Mckee, C. Harding, Angew. Chem., Int. Ed. 45 (2006) 7192.

[24] G. Fernandez, M. Corbella, G. Aullon, M. Maestro, J. Mahia, Eur. J. Inorg. Chem. (2007) 1285.

[25] J.P. Costes, F. Dahan, B. Donnadieu, M.I. Fernandez-Garcia, M.J. Rodriguez-Douton, Dalton Trans. (2003) 3776.

[26] V. Amendola, M. Boiocchi, B. Colasson, L. Fabbrizzi, M. Rodriguez-Douton, F. Ugozzoli, Angew. Chem., Int. Ed. 45 (2006) 6920.

[27] P.A. Gale, S.E. Garcia-Garrido, J. Garric, Chem. Soc. Rev. 37 (2008) 151.

[28] J.P. Costes, B. Donnadieu, R. Gheorghe, G. Novitchi, J.P. Tuchagues, L. Vendier, Eur. J. Inorg. Chem. (2008) 5235.

[29] M. Maneiro, M.R. Bermejo, A. Sousa, M. Fondo, A.M. Gonzalez, A. Sousa-Pedrares, C.A. McAuliffe, Polyhedron 19 (2000) 47.

[30] M. Maneiro, M.R. Bermejo, M.I. Fernandez, E. Gomez-Forneas, A.M. Gonzalez-Noya, A.M. Tyryshkin, New J. Chem. 27 (2003) 727.

[31] G.M. Sheldrick, in: SHELX-97 (SHELXS 97 and SHELXL 97), Programs for Crystal Structure Analyses, University of Göttingen, Germany, 1998.

[32] G.M. Sheldrick, in: SADABS, Program for Scaling and Correction of Area Detector Data, University of Göttingen, Germany, 1996.

[33] W.J. Geary, Coord. Chem. Rev. 7 (1971) 81.

[34] D. Kong, Y. Xie, Inorg. Chim. Acta 338 (2002) 142.

[35] J.A. Bonadies, M.L. Maroney, V.L. Pecoraro, Inorg. Chem. 28 (1989) 2044.

[36] V. Daier, D. Moreno, C. Duhayon, J. Tuchagues, S. Signorella, Eur. J. Inorg. Chem. (2010) 965.

[37] M.-N. Collomb, C. Mantel, S. Romain, C. Duboc, J.-C. Leprêtre, J. Pécaut, A. Deronzier, Eur. J. Inorg. Chem. (2007) 3179.

[38] D. Pursche, M.V. Triller, C. Slinn, N. Redding, A. Rompel, B. Krebs, Inorg. Chim. Acta 357 (2004) 1695.

[39] C. Bouchameni, C. Beghidja, A. Beghidja, P. Rabu, R. Welter, Polyhedron 30 (2011) 1774.

[40] E.C. Constable, C.E. Housecroft, P. Kopecky, E. Schonhofer, J.A. Zampese, CrystEngComm. 13 (2011) 2742.

[41] H.A. Habib, Polyhedron 29 (2010) 2537.

[42] P. Przychodzen, M. Rams, C. Guyard-Duhayon, B. Sieklucka, Inorg. Chem. Commun. 8 (2005) 350.

[43] N. Matsumoto, Z.J. Zhang, H. Okawa, S. Kida, Inorg. Chim. Acta 160 (1989) 153.

[44] H. Miyasaka, R. Clérac, T. Ishii, H.-C. Chang, S. Kitagawa, M. Yamashita, J. Chem. Soc., Dalton Trans. (2002) 1528.